J|A|C|S
ARTICLES
Published on Web 06/22/2006

Designed High Affinity Cu^{2+}-Binding α-Helical Foldamer

Andrew J. Nicoll,[†] David J. Miller,[†] Klaus Fütterer,[‡] Raymond Ravelli,[§] and Rudolf K. Allemann*,[†]

Contribution from the School of Chemistry, Cardiff University, Main Building, Park Place, Cardiff, CF10 3AT, UK, School of Biosciences, University of Birmingham, Edgbaston, Birmingham, B15 2TT, UK, and EMBL Outstation, 6 rue Jules Horowitz, 38042, Grenoble Cedex 9, France

Received March 18, 2006; E-mail: allemannrk@cf.ac.uk

Abstract: The design, synthesis, and characterization of a folded high-affinity metal-binding peptide is described. Based on the previously described folded peptide NTH-18, in which an α-helix was constrained through two disulfide bonds to a C-terminal extension of noncanonical secondary structure, a peptide (**1**) was designed to contain two histidine residues in positions 3 and 7. Air oxidation of **1** led to the formation of peptide **2**, which contained two intramolecular disulfide bonds. The presence of the two histidines significantly destabilized the α-helical structure of **2** when compared to NTH-18. However, CD spectroscopy revealed that the addition of certain transition metal ions allowed the reformation of a stable α-helix. CD, NMR, and EPR spectroscopy as well as MALDI-TOF mass spectrometry indicated that **2** bound to Cu^{2+} to form a 1:1 complex via the imidazoles of the two histidine side chains. A glycine displacement assay revealed a dissociation constant for this complex of 5 nM at pH 8, which is the lowest reported value for a designed Cu^{2+}-binding peptide. This peptide displayed more than 100-fold selectivity for Cu^{2+} over Zn^{2+}, Ni^{2+}, and Co^{2+}. The 1.05 Å crystal structure of the Cu(II)-complex of **2** revealed a square-pyramidal coordination geometry and confirmed that **2** bound to copper in an α-helical conformation via its two histidine side chains. The high affinity metal binding of peptide **2** demonstrates that metals can be used for the selective nucleation of α-helices.

Introduction

The specific interaction of proteins with nucleic acids or with other proteins often relies on the accurate presentation of amino acid residues on the surface of α-helices. Despite their relative abundance as recognition elements, isolated α-helices display often only marginal stability and the specificity and affinity of the biological interactions depend on the presence of the remainder of the protein. The low stability of isolated α-helices normally prevents their use as tools for targeted intervention in biological systems. Recently, methods have been developed for the stabilization of α-helical segments of proteins through their introduction into small, natural polypeptides of high intrinsic stability. The relatively stable pancreatic polypeptide has been used to produce catalytically active miniature enzymes,[1−3] to present in a miniature DNA binding protein several of the DNA contacting residues of the recognition α-helix of the homeodomain protein engrailed[4−7] and to target the surface of proteins.[8] Similarly, the 18-residue neurotoxic peptide apamin allowed the generation of a miniature oxaloacetate decarboxylase, the activity of which could be controlled through alterations of the redox conditions.[9]

In addition to interactions with other elements of secondary structure within globular proteins, nature also uses metal ions to stabilize α-helices. Metals often bind to two or more nitrogen atoms of the imidazole ring of histidines. For instance, Zn-fingers rely on metal coordination to bind with high affinity and specificity to DNA through an α-helical recognition sequence.[10] Several designed, short synthetic peptides have been reported in which metal coordination led to helix stabilization.[11−16] The first peptides for which metal-induced α-helical stabilization was reported bound to transition metals with affinities in the mid-micromolar range and with undefined metal coordination.[11] These peptides displayed significant α-helical character even in the absence of metal ions, and the helical stabilization observed was therefore only modest. [Pd(II)-$NH_2(CH_2)_2NH_2$]-stabilized α-helical turns[12−14] were used to induce α-helicity

[†] Cardiff University.
[‡] University of Birmingham.
[§] EMBL Outstation.

(1) Taylor, S. E.; Rutherford, T. J.; Allemann, R. K. *Bioorg. Med. Chem. Lett.* **2001**, *11*, 2631.
(2) Taylor, S. E.; Rutherford, T. J.; Allemann, R. K. *J. Chem. Soc., Perkin Trans. 2* **2002**, 751.
(3) Nicoll, A. J.; Allemann, R. K. *Org. Biomol. Chem.* **2004**, *2*, 2175.
(4) Montclare, J. K.; Schepartz, A. *J. Am. Chem. Soc.* **2003**, *125*, 3416.
(5) Zondlo, N. J.; Schepartz, A. *J. Am. Chem. Soc.* **1999**, *121*, 6938.
(6) Chin, J. W.; Schepartz, A. *J. Am. Chem. Soc.* **2001**, *123*, 2929.
(7) Guerrero, L.; Smart, O. S.; Woolley, G. A.; Allemann, R. K. *J. Am. Chem. Soc.* **2005**, *127*, 15624.
(8) Gemperli, A. C.; Rutledge, S. E.; Maranda, A.; Schepartz, A. *J. Am. Chem. Soc.* **2005**, *127*, 1596.
(9) Weston, C. J.; Cureton, C. H.; Calvert, M. J.; Smart, O. S.; Allemann, R. K. *ChemBioChem* **2004**, *5*, 1075.
(10) Allemann R. K. *Encyclopedia of Molecular Biology*; Creighton, T. E., Ed.; Wiley: New York, 1999; pp 2586−2593.
(11) Ghadiri, M. R.; Choi, C. *J. Am. Chem. Soc.* **1990**, *112*, 1630.
(12) Kelso, M. J.; Hoang, H. N.; Appleton, T. G.; Fairlie, D. P. *J. Am. Chem. Soc.* **2000**, *122*, 10488.
(13) Kelso, M. J.; Hoang, H. N.; Oliver, W.; Sokolenko, N.; March, D. R.; Appleton, T. G.; Fairlie, D. P. *Angew. Chem., Int. Ed.* **2003**, *115*, 437.

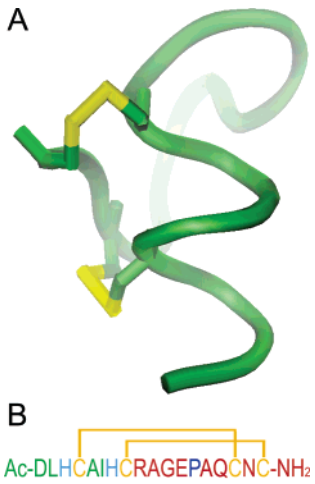

Figure 1. (a) Three-dimensional structure of the NTH-18,[18] indicating the two disulfide bonds that stabilize the C-terminal α-helix. (b) Amino acid sequence of **1** showing helical region (green), residues involved in metal chelation (light blue), cysteines involved in intramolecular disulfide bond formation (orange), and the turn-forcing proline (blue). The crossed disulfide pattern shown is that of peptide **2**, while, in **3** (not shown), the disulfide bonds are parallel and formed between cysteines 4 and 18 and 8 and 16, respectively.

in short peptide fragments of the metalloprotease thermolysin.[13] While the solution structure of these stabilized peptides was solved rigorously by NMR spectroscopy, the coordination geometry of the metal was not determined and no binding affinities were reported. These peptides are a remarkable manifestation of a high level of success in the design of metalloproteins of three-dimensional structure. However, the metal binding affinities of these peptides are in the micro- to millimolar range, well short of those typically found in natural proteins and required for biological applications. One example where sub-micromolar affinities were reported was a lanthanide binding tag.[17] This chemically evolved small peptide was designed from the Ca^{2+}-binding EF-hand motif of troponin C and bound to rare earth metal ions with affinities between 62 and 3500 nM. The lanthanide ions were coordinated by oxygens from side chain carboxylates and backbone carbonyls, and hence only modest affinities would be expected for transition metal ions such as copper, nickel, or zinc.

The metal-induced transition from a largely unfolded peptide chain to a stable α-helical structure is hindered by the entropic cost of protein folding. Reducing this negative entropy change, which necessarily limits the potential stability of metal−peptide complexes, inherently leads to tighter binding. We have previously reported the design of the 18-residue polypeptide NTH-18, in which an α-helix was constrained through two disulfide bonds to a C-terminal extension of noncanonical secondary structure (Figure 1A).[18] In its oxidized form, NTH-18 displayed significant stability to heat and changes of pH. The secondary structure of the peptide remained largely unchanged for temperatures up to 80 °C and pH values as low as 2. Despite its high stability, the solution NMR structure of NTH-18 indicated that, while the α-helix was well defined between residues 3 and 8, the definition of the two amino acid residues at either end of the α-helix was poor. Here we report the synthesis of a high affinity Cu^{2+}-binding peptide (**2**), which was based on NTH-18, and describe its X-ray crystal structure at 1.05 Å resolution.

Results and Discussion

Design and Synthesis of Peptide 1. For the design of **1**, two histidine residues replaced the solvent exposed Gln 3 and Lys 7 of NTH-18 (Figure 1).[19] The presence of the histidines was envisaged to lead to the generation of a metal-dependent α-helical switch, since histidines normally have a destabilizing effect on α-helices, while glutamines and lysines are helix-stabilizing.[19] Their introduction was expected to reduce the α-helical character of the peptide. However, the spacing of the two histidines of approximately one α-helical turn apart implied that they might be ideally placed to promote helix formation through coordination of transition metal ions such as Cu^{2+}.

1 was synthesized on a solid support using fluorenylmethoxycarbonyl (Fmoc) chemistry. The peptide was purified by HPLC to greater than 98% purity, and its identity was confirmed by MALDI-TOF mass spectrometry. The experimentally determined mass was 1981.5, which agreed well with the theoretical mass of 1981.3 for the fully reduced peptide. As had been observed for NTH-18, air oxidation of the reduced peptide in 10% DMSO at pH 8 yielded two products of identical mass that were easily separated by reversed phase HPLC (Supporting Information). For NTH-18, these two forms could be assigned to the peptides with crossed and parallel patterns of the disulfide bonds.[18] CD spectroscopy indicated that the more polar peptide (**2**) had the higher α-helical content (Figure 2), while the solution of the X-ray crystal structure of its Cu(II) complex confirmed the presence of a crossed disulfide pattern (vide infra) where disulfide bonds linked cysteines 4 and 16 and 8 and 18, respectively (Figure 1). In analogy to NTH-18, the less polar peptide (**3**) was assumed to contain a parallel disulfide pattern with disulfide bonds between cysteins 4 and 18 and 8 and 16.

CD Spectroscopy. The secondary structures of **2** and **3** and their Cu(II) complexes were characterized by CD spectroscopy. The mean residue ellipticities at 222 nm, $[\Theta]_{r,222}$, of −8240 and −5200 deg cm^2 dmol^{-1} residue^{-1} measured for the two metal-free peptides corresponded to approximately 26% and 17% α-helix.[9] This was significantly less than the values of 44% and 26% that had been observed for the crossed and parallel versions of NTH-18 confirming the strong helix-destabilizing effect of the two histidines.[18]

While the addition of $CuSO_4$ to a solution of **3** resulted in only a small change in its CD spectrum, a strong decrease of the mean residue ellipticity at 222 nm of **2** was observed upon addition of the metal ions (Figure 2). After the addition of 1 equiv of metal ion to a solution of **2**, no further change in the CD spectrum was observed suggesting the formation of a 1:1 complex between **2** and Cu^{2+} (Figure 2B). The formation of a 1:1 complex between **2** and Cu^{2+} was confirmed by MALDI-TOF mass spectrometry (vide infra).

The isodichroic point observed in the CD-titration experiments at 204 nm suggested a two-state equilibrium between

(14) Kelso, M. J.; Beyer, R. L.; Hoangt, H. N.; Lakdawala, A. S.; Snyder, J. P.; Oliver, W. V.; Robertson, T. A.; Appleton, T. G.; Fairlie, D. P. *J. Am. Chem. Soc.* **2004**, *126*, 4828.
(15) Kharenko, O. A.; Ogawa, M. Y. *J. Inorg. Biochem.* **2004**, *98*, 1971.
(16) Ghosh, D.; Pecoraro, V. L. *Inorg. Chem.* **2004**, *43*, 7902.
(17) Nitz, M.; Sherawat, M.; Franz, K. J.; Peisach, E.; Allen, K. N.; Imperiali, B. *Angew. Chem., Int. Ed.* **2004**, *43*, 3682.
(18) Nicoll, A. J.; Weston, C. J.; Cureton, C.; Ludwig, C.; Dancea, F.; Spencer, N.; Günther, U. L.; Smart, O. S.; Allemann, R. K. *Org. Biomol. Chem.* **2005**, *3*, 4310.
(19) O'Neil, K. T.; Degrado, W. F. *Science* **1990**, *250*, 646.

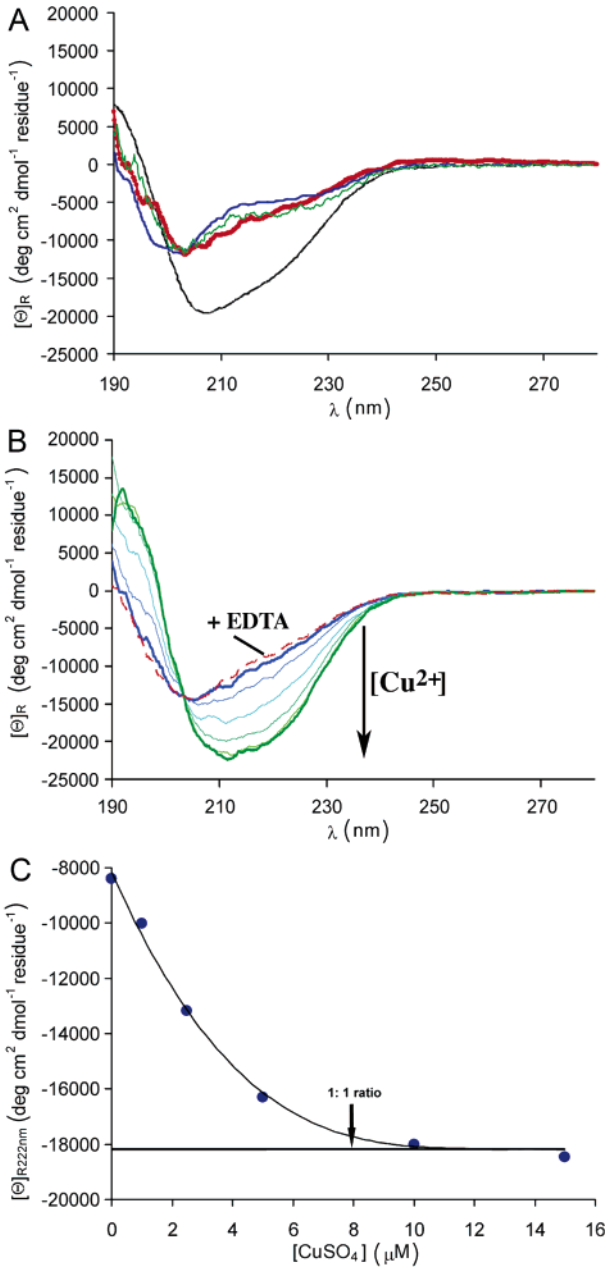

Figure 2. (a) Comparison of the CD spectra of NTH-18 (black line),[18] TCEP-reduced **1** in the presence of 15 μM $CuSO_4$ (red), and **3** in the presence (50 μM) (green) and absence (blue) of $CuSO_4$ in 5 mM potassium phosphate buffer (pH, 7.0). (b) CD spectra of **2** (8 μM) in the presence of 0, 1, 2.5, 5, 10, and 15 μM $CuSO_4$ in 5 mM potassium phosphate buffer (pH, 7.0). CD spectrum of **2** in the presence of 15 μM $CuSO_4$ and 15 μM EDTA (red intermittent line) is also shown. (c) Mean residue ellipticity at 222 nm from the CD spectra of **2** in (b) as a function of the concentration of $CuSO_4$ indicating a 1:1 binding mode.

free **2** and its Cu(II) complex (Figure 2B). The shape of the CD spectrum of the Cu(II) complex of **2** was that typically observed for peptides with a substantial content of α-helix with minima of −20 600 and −18 500 deg cm^2 $dmol^{-1}$ $residue^{-1}$ at 208 and 222 nm, respectively, and a maximum of 13 300 deg cm^2 $dmol^{-1}$ $residue^{-1}$ at 192 nm. From the value of $[\Theta]_{r,222}$, an α-helical content of 58% could be estimated suggesting that the 10 N-terminal residues were in an α-helical conformation. The addition of EDTA to a solution of the Cu(II) complex of **2** resulted in a CD spectrum identical to that of metal-free **2**. Reduction of the disulfide bonds of **2** with 2,2,2-tris-carboxyethyl phosphine (TCEP) led to a CD spectrum indicative of a random coil-like structure. The spectrum of reduced **2** was unaltered by the addition of $CuSO_4$ suggesting a central role for the disulfide bonds for both structure and metal binding.

Magnetic Resonance Spectroscopy of Cu(II) Binding by 2. The pK_a values of the two imidazole histidines of **2** were determined by ^{1}H NMR spectroscopy in D_2O. The chemical shifts of the nonlabile imidazole protons of His-3 and His-7 were measured over more than five pH units (pH* 4.5 to 9.7) leading to two titration curves with midpoints of 6.9 and 7.0 (Supporting Information). These pK_a values, which had been measured in D_2O, were not corrected for isotope effects. In agreement with the CD experiments of unliganded **2**, these values were suggestive of a poorly defined secondary structure in the vicinity of the histidines, since charge repulsion between spatially close histidines normally results in the depression of their pK_a values.[3,20] Addition of increasing concentrations of $CuSO_4$ to **2** in D_2O led to significant broadening of the signals for the protons on C2 and C5 of the histidines at 8.4 and 7.2 ppm. While some line broadening was also observed for the other NMR signals, the increased effect from the addition of the paramagnetic metal ions on the protons of the imidazoles of the two histidines suggested that Cu^{2+} bound to **2** via these residues (Figure 3A).

Metal coordination of **2** was further investigated by EPR spectroscopy (Figure 3B). The spectrum of the Cu(II) complex of a 178 μM solution of **2** was indicative of a classic type-II copper center, suggesting a square planar, square pyramidal, or Jahn−Teller distorted octahedral metal center.[21] A hyperfine splitting value of 166×10^{-4} cm^{-1} and a $g_{||}$ of 2.302 excluded coordination via sulfur and indicated that the metal bound to N- and O-ligands.[21] These observations together with the NMR, CD, and MS data indicated that **2** formed a 1:1 complex with the metal most likely through coordination to the imidazoles of His 3 and His 7 together with additional ligands from either the solvent or other side chains of the peptide.

At concentrations of **2** in excess of 2 mM, the value for $g_{||}$ decreased slightly to 2.26 while $A_{||}$ increased to 186×10^{-4} cm^{-1} (Figure 3C). In addition, superhyperfine splitting was observed in the perpendicular component of the spectrum, which could however not be accurately measured due to the observed overlap between the parallel and perpendicular component of the spectrum. The spin Hamiltonian parameters are consistent with metal binding through nitrogen ligands for peptide concentrations above 2 mM.[22] These results suggested that at elevated concentrations (>2 mM) a 2:1 complex was formed where two peptides bound to the metal, most likely through the four histidines.

X-ray Crystal Structure of Cu(II) Complex of 2. The crystal structure of the Cu(II) complex of **2**, which was solved by single wavelength anomalous dispersion to a resolution of 1.05 Å, revealed the details of the interaction. The crystal lattice (space group $P6_322$) with hexagonal symmetry (space group $P6_322$) contained two crystallographically distinct polypeptide chains (chains A and B) that experienced different crystal packing contacts and were built and refined independently of

(20) Broo, K. S.; Brive, L.; Ahlberg, P.; Baltzer, L. *J. Am. Chem. Soc.* **1997**, *119*, 11362.
(21) Sakaguchi, U.; Addison, A. W. *J. Chem. Soc., Dalton Trans.* **1979**, 600.
(22) Pilbrow, J. R. *Transition ion electron paramagnetic resonance*; Clarendon Press: Oxford, 1990.

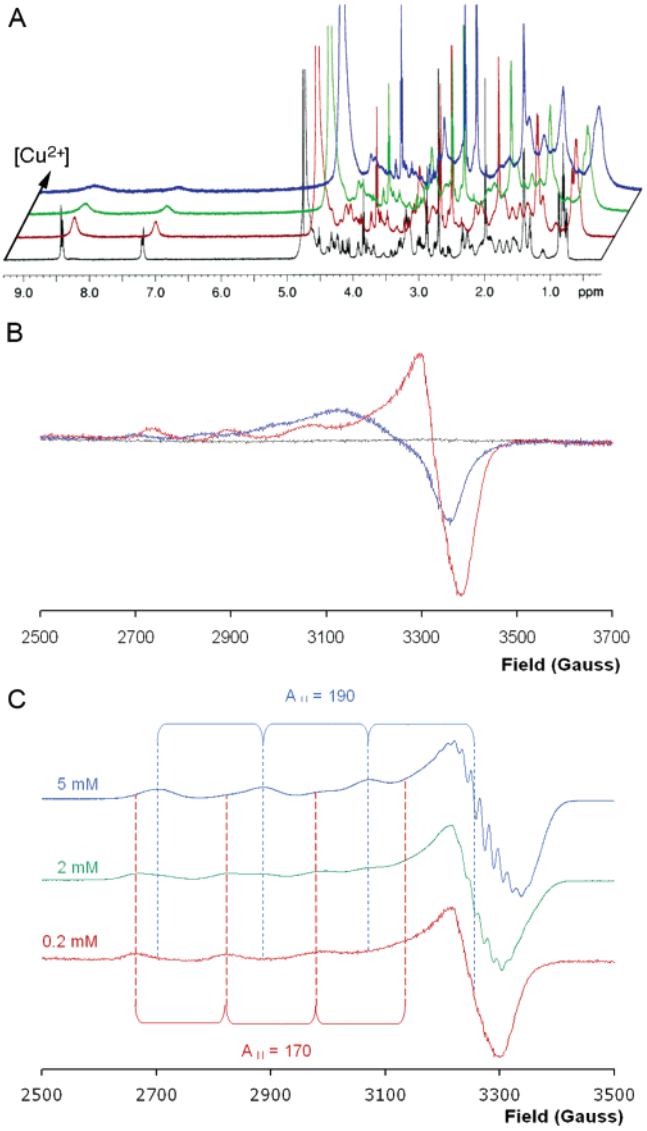

Figure 3. (a) ^{1}H NMR spectrum of **2** (178 μM) (black) and on addition of 0.05 (red), 0.1 (green), and 0.15 equiv (blue) of $CuSO_4$ in D_2O (100 mM potassium phosphate buffer pH* 6.1, 30 °C). (b) EPR spectra of $CuSO_4$ (blue) (pH 7, unbuffered), **2** (178 μM) (black), and the Cu complex of **2** (red) complex (pH 7, 5 mM potassium phosphate buffer). (c) EPR spectra of the Cu(II) complex of **2** for increasing concentrations of peptide ([**2**] = 200 μM (red), 2 mM (green), and 5 mM (blue)) in 5 mM potassium phosphate, pH 7.

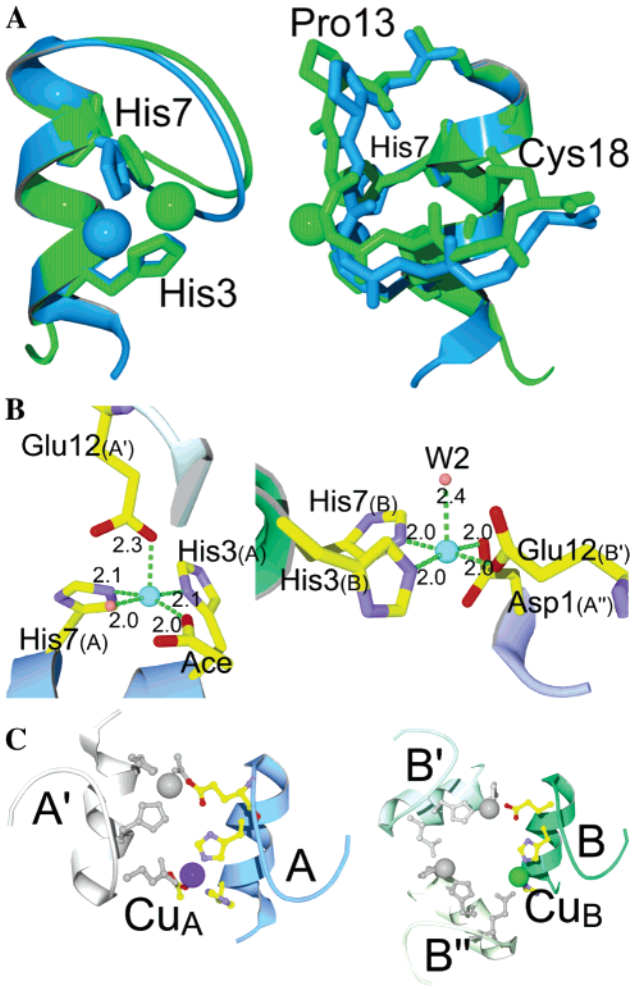

Figure 4. (a) Two orthogonal views of the superimposed Cu(II) complex of **2** peptides highlighting the well-defined helix (left) and the disordered loop (right). Ribbons are colored blue (chain A) and green (chain B). (b) Metal coordination in Cu(II)−**2**. Cu_A and Cu_B sites are shown on the left and right, respectively. Distances are indicated in Å. Capital labels in parentheses refer to chains A and B, with primed labels denoting symmetry-related chains. Amino acid side chains are depicted as sticks colored according to atom type (yellow = carbon, blue = nitrogen, red = oxygen). Water molecules in pale red spheres, and Cu (turquoise) as spheres with arbitrary radii. The solvent acetate is denoted with Ace. (c) Metal-mediated crystal contacts. Views along the 2-fold (left) and 3-fold (right) rotation axes in Cu(II)-**2**. Symmetry-related peptide chains are denoted by (primed) capital letters.

each other (Supporting Information). Nevertheless, the backbone conformations of the two chains were similar (Figure 4A) showing a root-mean-square deviation of 0.5 Å for the 18 Cα atoms of the full-length peptide and 0.3 Å with respect to the nine α-helical residues. Both chains displayed a N-terminal α-helix capped with a loop formed by residues Gly 11 to Gln 15. Two crossed disulfide bridges from Cys 4 to Cys 16 and from Cys 8 to Cys 18 connected the α-helix to the extended C-terminal peptide segment. Small conformational differences were observed for the geometry of the disulfide bridges between cysteines 4 and 16, the capping loop, and the C-terminal end of **2** (Figure 4A). However, the most striking differences between chains A and B were seen in the metal binding site and the conformation of the N-terminal Asp. In chain A, Asp 1 and the N-terminal-capping acetyl group participated in the canonical H-bond pattern of the helix, whereas, in chain B, the latter groups were rotated by 180° about the Cα−C bond of Asp 1 relative to the conformation seen in chain A. As a result, the α-helical geometry extended only to Leu 2 in chain B. This difference in conformation, in part, is explained by the fact that Asp 1 of chain A participates in the coordination polyhedron of one of the Cu sites.

Chains A and B had similar but distinct Cu sites, Cu_A and Cu_B, which were both coordinated by five ligands in a square-pyramidal fashion (Figure 4B). His 3 and His 7 of chain A, an acetate ion from the crystallization buffer, and a water molecule formed the base of the pyramid, while Glu 12 (from a symmetry-related chain A) coordinated Cu_A axially. The metal−ligand distances ranged from 2.00 to 2.10 Å (average 2.04 Å) in the basal plane and measured 2.25 Å to the apical position. Two symmetry-related B chains and one chain A were involved in the coordination of Cu_B. Here a water molecule occupied the apical position, while the corners of the basal plane were formed

by the side chains of His 3 and His 7 of chain B, Glu 12 of a symmetry-related chain B, and Asp 1 of chain A. The apical position was 2.43 Å away from the metal site, while metal−ligand distances lay between 1.98 and 2.01 Å in the basal plane (average 2.00 Å), indicating a slightly more regular coordination polyhedron than was observed for the Cu_A site.

The observation of metal-mediated peptide−peptide contacts in the three-dimensional lattice (Figure 4C) raises the question whether Cu^{2+}-bound **2** might form metal-mediated dimers or trimers in solution. At submillimolar concentrations of **2** the CD-titration (Figure 2) and the EPR experiments (Figure 3) described suggested that one molecule of **2** bound to one copper ion. However, EPR had also indicated that at millimolar concentrations of **2** copper mediated dimers might form. The metal-mediated contacts observed in the crystal made up only a subset of the packing contacts, most of which were formed by direct peptide−peptide interactions (supplementary information) in the crystal lattice of the Cu complex of **2**. This suggests that the formation of the crystal lattice is driven by direct peptide−peptide interactions rather than metal-mediated contacts. Given that solvent molecules (H_2O, acetate) can be recruited to help complete the Cu-coordination polyhedron, as observed in the present crystal structure of Cu−**2**, our data suggest that proper Cu-coordination by **2** is not dependent on formation of dimers or higher oligomers. Nonetheless, higher assembly states were suggested by the EPR experiments at high peptide concentrations, which would reflect the dense packing of molecules in the crystal lattice. MALDI-TOF mass spectrometry confirmed the 1:1 stoichiometry of the Cu(II) complex of **2** in solution that had been observed by CD and EPR spectroscopy for concentrations of **2** below 2 mM. No trace of dimer or trimers was detected in the MADI-TOF MS of Cu(II) bound **2** at 1 mM concentration (Supporting Information). The isotopic distribution measured in the MALDI-TOF mass spectrum also confirmed the formation of a 1:1 complex and excluded the formation of higher oligomers or a 2:2 complex at the concentrations used (see Materials and Methods and Supporting Information).

Metal Ion Binding Affinities of 1. Because of the high affinity of **2** for Cu^{2+}, the binding constant could not be obtained from the CD-titration data. The stability of the complex was therefore determined in a glycine displacement assay.[23] The changes in the CD spectrum of a 8 μM solution of the Cu(II) complex of **2** resulting from the addition of increasing amounts of glycine were measured (Supporting Information). From the known stability of the glycine complex of Cu^{2+} of 3.388 μM,[24] the dissociation constant of the Cu(II) complex of **2** was calculated as 66 nM at pH = 7.0. The stability for the complex remained unchanged when the pH of the solution was reduced to 6.0, but the dissociation constant was reduced to 5 nM at pH 8.0, most likely as a consequence of the deprotonation of the imidazoles of the coordinating histidines. While histidines in an i, $i + 4$ spacing have been used before to stabilize peptides through binding to metal ions,[11,25,26] the dissociation constants reported here are reduced by more than 4 orders of magnitude and, to the best of our knowledge, represent the most stable Cu(II) complex of any designed peptide.

2 displayed substantial metal ion binding selectivity. The affinity of **2** for Ni^{2+} and Zn^{2+} was reduced by almost 3 orders of magnitude relative to Cu^{2+}. Dissociation constants of 10, 20, and 190 μM for the Zn(II), Ni(II), and Co(II) complexes of **2** could be obtained directly from titration experiments monitored by CD spectroscopy (Supporting Information). No binding to Mg^{2+} or Fe^{3+} was observed in the accessible concentration range up to 1 mM. The specificity of metal ion binding of **2** was therefore similar to that of imidazole.[24] The binding affinity, however, was increased by approximately 3 orders of magnitude. The exceptionally tight binding of **2** relative to imidazole [24] and previously reported helical switches[11] is most likely the consequence of the preorganization of metal-free **2** through the two disulfide bonds, which generates a peptide that adopts a relatively rigid conformation poised to bind metal ions, thereby reducing the entropic cost of the conformational reorganization accompanying metal binding. In agreement with this explanation, no binding of reduced **2** to Cu^{2+} was observed for metal concentrations as high as 15 μM.

In summary, an 18-residue foldamer **2** has been designed that binds selectively to transition metal ions with up to nanomolar affinity. On addition of metal ions, **2** undergoes a conformational change to a stably folded three-dimensional structure in which an α-helix is held in place through square-pyramidal metal coordination. Such metal-dependent foldamers may have applications as oxidation-state sensitive affinity tags, for the generation of artificial models of active sites of metalloproteins, and as reagents to selectively target interfaces involved in protein−protein and protein−nucleic acid interactions that often rely on α-helices for affinity and specificity to control many processes central to biology.

Materials and Methods

Peptide Synthesis and Purification. Reduced **1** was synthesized using an Applied Biosystems 433A automated peptide synthesizer and standard Fmoc protocols.[27] The Fmoc and side-chain protected amino acids (Asn, Cys, Gln, His (Trt); Asp, Glu (O*t*Bu); Phe, Ser, Tyr, Thr (*t*Bu); Lys (Boc) and Arg (Pbf)) were coupled to Fmoc-5-(4-aminomethyl-3,5-dimethoxyphenoxy) valeric acid on a poly(ethylene glycol) support. Prior to cleavage and deprotection with 10 mL of 2,2,2-trifluoroacetic acid (TFA)/water/phenol/triisopropylsilane (88:5:5:2; v/v) per gram of resin for 2 h at room temperature, reduced **1** was acetylated with acetic anhydride (0.5 M), diisopropylethylamine (125 mM), and *N*-hydroxybenzotriazole (15 mM) in *N*-methyl-pyrrolidinone using 2-(1*H*-benzotriazole-1-yl)-1,3,3,3-tetramethyluronium hexafluorophosphate for activation. The resin was removed by filtration, and the soluble products were concentrated in vacuo and precipitated by washing with 3 × 5 mL of ice-cold diethyl ether. The peptide was dissolved in 50 mL of 10% acetic acid followed by lyophilization. **1** was then redissolved in 10 mL of 0.05% TFA, purified by reversed-phase HPLC on a LUNA 10 μ C18 column (250 mm × 21.2 mm), and eluted with a linear gradient from 10% to 30% acetonitrile in water (0.05% TFA) with a flow rate of 10 mL min^{-1} over 60 min. Solvent was removed in vacuo followed by lyophylization. **1** was identified by MALDI-TOF mass spectrometry. The experimentally determined mass of 1981.5 agreed well with the calculated mass of 1981.3 for the protonated peptide. The purity of **1** was shown to be greater than 98% by HPLC on an analytical LUNA 10 μ C18 column (250 mm × 4.6 mm).

(23) Jones, C.; Abdelraheim, S.; Brown, D.; Viles, J. *J. Biol. Chem.* **2004**, *279*, 32018.
(24) Dawson, R. M. C.; Elliot, D. C.; Elliot, W. H.; Jones, K. M. *Data for Biochemical Research*; Claredon Press: Oxford, UK, 1986.
(25) Gelinsky, M.; Vahrenkamp, H. *Eur. J. Inorg. Chem.* **2002**, 2458.
(26) Shields, S. B.; Franklin, S. J. *Biochemistry* **2004**, *43*, 16086.
(27) Jones, J. *Amino Acid and Peptide Synthesis*; Oxford University Press: Oxford, 1992.

Oxidation of 1. Oxidation was performed in potassium phosphate buffer (5 mM, pH 8) to a final peptide concentration of less than 0.5 mg mL^{-1} to prevent oligomerization. **1** was treated with 2 equiv of 2,2,2-tris-carboxyethyl phosphine (TCEP) to ensure complete reduction. The peptide was stirred vigorously for 2 h before the addition of 10% DMSO to facilitate oxidation.[28] The reaction was left for 24 h to allow complete oxidation, after which water was removed in vacuo with gentle heating. The two products (**2** and **3**) (Figure S1) were separated by preparative HPLC using a LUNA 10 μ C18 column (250 mm × 21.2 mm). HPLC analysis on an analytical LUNA 10 μ C_{18} column (250 mm × 4.6 mm) revealed that the two isomers had been fully separated.

CD Spectroscopy. Experiments were performed using a Jasco J-810 spectropolarimeter with 1−10 μM solutions of peptides in a 5 mm cuvette (20 °C, 5 mM potassium phosphate buffer, pH 6−8).

Metal binding experiments were performed by addition of concentrated stocks of $CuSO_4$ (1−100 μM) to peptide solutions. Glycine displacement was carried out for the Cu(II) complex of **2** by titration of glycine from concentrated stocks and the displacement monitored by the change in the mean residue ellipticity at 222 nm (see Supporting Information). Metal binding of **2** was then compared to published absolute stability constants (K_{1Cu}) of the glycine−copper complex,[24] using the following equations:[23]

$$\log \alpha = pK_a - pH$$

$$\log K_{app} = \log K_1 - \log \alpha$$

and

$$\log K_{app,pH} = \log K_1 - \log \alpha,$$

and with $pK_a = 9.63$ and $\log K_{1Cu} = 8.1$, a value of 5.47 is calculated for $\log K_{app,pH7,Cu}$ (or 2.95×10^5 M^{-1} for $K_{app,pH7,Cu}$).

The dissociation constant K_D was then calculated as

$$K_D = (1/K_{app,pH\ 7,Cu})[\text{glycine}]_{1/2}/[\mathbf{2}]$$

The concentration of glycine required to displace half of the ligand from the Cu(II) complex of **2**, $[\text{glycine}]_{1/2}$, was obtained using SigmaPlot from the graph of the change of the mean residue ellipticity at 222 nm as a function of the concentration of glycine (see Supporting Information).

Similarly, the dissociation constant of the Ni(II) complex of **2** was calculated from glycine displacement assays using $K_{app,pH\ 7,Ni} = 1.2 \times 10^3$ M^{-1}.[24] The K_D value 8.1 μM obtained in this manner compared well with that obtained directly from titration experiments monitored by CD spectroscopy.

MALDI-TOF Mass Spectrometry. MALDI-TOF mass spectrometry experiments were performed in positive ion mode on a Micromass MALDI micro MX instrument. All spectra were measured in reflectron mode using a nitrogen laser at 337 nm. The matrix used was α-cyano-4-hydroxycinnamic acid. Pure peptide samples were dissolved in deionized water (0.1% TFA), while the analysis of the metal complexes was performed in 5 mM NH_4HCO_3. To ensure the 1:1 complex observed in the mass spectra of 1 mM Cu^{2+} and 1 mM **2** was not due to the formation of Cu^{2+} adducts, these spectra were also run in the presence of 10 and 240 mM NaCl (Supporting Information).

NMR Spectroscopy of 2. Copper titration experiments were performed on a Bruker Avance 500 MHz spectrometer with **2** (1 mM, 50 mM potassium phosphate, pH* 6) in D_2O and after the addition of 0.05, 0.1, and 0.15 equivalents of $CuSO_4$ at 30 °C.

NMR titrations for the determination of the pK_a values of the histidines in **2** were performed at 290 K using 6.0 mM **2** in D_2O on a Bruker AC 300 MHz spectrometer. The chemical shifts of the H2 and H4 protons of the imidazole rings of His 3 and His 7 were measured as a function of pH* (uncorrected) with the assumption that the isotope effects cancel out (Figure S3).[20] The pK_a values were determined from the titration curves by fitting curves describing the titration of a monoprotic acid. The pH* of the solution was adjusted through the addition of 100 mM NaOD.

EPR Spectroscopy. EPR spectra of $CuSO_4$ (178 μM, pH 7, 10% glycerol) and Cu−**2** (178 μM, *p*H 7, 5 mM potassium phosphate, 10% glycerol) were recorded using a Bruker BioSpin EMX spectrometer at 100 K using an ER 4131 VT temperature controller. A 9.922 mW microwave power at a frequency of 9.379 GHz was used with a modulation amplitude of 4.00 G and frequency of 100 kHz. All spectra were recorded with a sweep width of 1000 G centered at 3000 G. The higher concentration EPR spectra were recorded at concentrations of 2 and 5 mM **2** and 2 mM $CuSO_4$ in 5 mM potassium phosphate, pH 7, containing 10% glycerol.

X-ray Crystallography. Crystals of Cu-bound **2** (5 mM, unbuffered) were obtained in a sparse matrix screen (Hampton Research Crystal Screen), growing over a reservoir of 20 mM $CaCl_2$, 100 mM sodium acetate (pH 4.6), and 30% v/v 2-methyl-2,4-pentanediol (MPD). Crystals were mounted in nylon loops from the original screen and frozen in liquid nitrogen without further treatment. Crystals were in space group $P6_322$, and diffraction data to 1.05 Å were recorded on station ID14-4 (ESRF Grenoble) at a wavelength of 0.9786 Å using inverse beam geometry (Table S1). Data were reduced using MOSFLM/SCALA.[29,30] The Matthews volume (2.18 $Å^3$/Da) indicated the presence of two peptide molecules per asymmetric unit. The anomalous signal was sufficient to locate two copper sites using SOLVE.[31] Phases were refined using SHARP [32] and solvent-flattened using SOLOMON[33] resulting in an electron density map of superb quality. A model comprising two peptide chains was built manually in O[33] and refined using REFMAC5 [34] with phase restraints. Inspection of the σ_A-weighted F_o-F_c map revealed strong negative density at the Cu_A site, and the occupancy was adjusted manually to 0.7 so as to minimize the free *R*-factor and to reduce residual density to noise level. The model was refined to a free *R*-factor of about 22%, at which point water molecules were added. Eventually, the model was refined using anisotropic thermal displacement parameters to a final free *R*-factor of 17.2% (R_{cryst} 15.9%). Release of the geometrical restraints led to a further decrease of free *R* to 15.6% (R_{cryst} 13.9%, ratio of observables to refined parameters of 4.6), but the restrained and unrestrained models were virtually identical with an RMSD of 0.04 Å for 256 peptide atoms. The final model of the Cu(II)-bound **2** peptide structure comprises 2 peptide chains (residues 1−18), 2 Cu sites, and 42 water molecules. Density for the side chain of Arg 9 was missing.

The coordinates of the copper complex of **2** have been deposited (CCDC entry: 611606).

Acknowledgment. This work was supported financially by the BBSRC and the EPSRC (studentship to A.J.N.). The authors would like to acknowledge the support of Dr. Damien Murphy, Dr. Paul Anderson, and Terry Green with EPR and Dr. Neil Spencer with NMR spectroscopy. The help of Dr. Scott White with X-ray data collection is gratefully acknowledged. Access to beamline ID14-4 at ESRF Grenoble was granted under Proposal MX-405.

(28) Tam, J. P.; Wu, C. W.; Liu, W.; Zhang, J. *J. Am. Chem. Soc.* **1991**, *113*, 6657.

(29) Leslie, A. G. W.; Brick, P.; Wonacott, A. *Daresbury Laboratory Information, Quarterly for Protein Crystallography* **1986**, *18*, 33−39.
(30) Collaborative Computational Project, Number 4. The CCP4 suite: programs for protein crystallography. *Acta Crystallogr., Sect. D* **1994**, *50*, 760.
(31) Terwilliger, T. C.; Berendzen, J. *Acta Crystallogr., Sect. D* **1999**, *55*, 849.
(32) De La Fortelle, E.; Bricogne, G. *Methods Enzymol.* **1997**, *276*, 472.
(33) Abrahams, J. P.; Leslie, A. W. G. *Acta Crystallogr.* **1996**, *D52*, 30.
(34) Jones, T. A.; Zou, J. Y.; Cowan, S. W.; Kjeldgaard, M. *Acta Crystallogr., Sect. A* **1991**, *47*, 110−119.

Supporting Information Available: HPLC trace of oxidized **1**, CD spectra of glycine displacement assays, CD spectra and binding curves for titrations of **2** with Ni(II), Zn(II), and Co(II) titrations curves for the measurements of the pK_a values of the histidines of **2**, mass spectra of the copper complex of **2**, crystal packing of Cu^{2+}-bound **2**, and X-ray data collection and refinement statistics. This material is available free of charge via the Internet at http://pubs.acs.org.

JA061513U